

# From Representations to Applications



# From Representations to Applications

Posters



# Determination of Discrete Sampling Grids with Optimal Topological and Spectral Properties

Luis Ibáñez, Chafiaâ Hamitouche, Christian Roux

Département Image et Traitement de l'Information  
ENST - Bretagne, Technopôle de Brest-Iroise  
BP 832 , 29285 Brest, France  
E-mail:Chafiaa.Hamitouche@enst-bretagne.fr

**Abstract.** This paper proposes 2D, 3D and 4D discrete sampling grids with optimal topological and spectral properties. It is shown here that those grids have advantages with respect to the classically used  $\mathbb{Z}^n$  grid. The proposed 3D grids are used to achieve surface extraction from volume data. Results are shown for a medical imaging application.

**Keywords:** Multidimensional discrete sampling, Compact Grids, 3D topology.

## 1 Introduction

Multidimensional signal processing often uses discrete sampling grids obtained as the tensor product of one-dimensional sampling grids. In a  $N$ -D space, the points of the  $\mathbb{Z}^n$  space are used as the natural sampling grid. It is shown here that this is not the best choice, because it makes very difficult to define a correct topology on it [1][2][10][12] and it oversamples the signal [11]. In this paper, we propose to construct optimal sampling grids, based on the compact spherical packing lattice concept well referenced in the geometry, information theory and solid state physics fields [6][5][3]. The obtained grids have interesting topological properties, that makes easier to solve the problem of surface extraction from volume data, which is extensively treated in the image processing area for the  $\mathbb{Z}^3$  sampling grid.

## 2 Determination of topologically optimal grids

### 2.1 Notions

**Voronoi region:** Given a  $N$ -dimensional grid (or "lattice") The Voronoi region  $V(\bar{x}, \bar{p}_i)$  of a grid point  $\bar{p}_i$  is defined as [8]:

$$V(\bar{x}, \bar{p}_i) = \{\bar{x} \in \mathbb{R}^n : \|\bar{x} - \bar{p}_i\| \leq \|\bar{x} - \bar{p}_j\| \quad \forall j \neq i\}$$

where the  $\bar{p}_j$  are the others grid points. The Voronoi region or Voronoi cell of a regular lattice, fills the  $N$ -D space by simple tilling. For the  $\mathbb{Z}^n$  grid, the Voronoi region is a  $N$ -D cube.

**Covering radius:** When a multidimensional sphere is replicated in a grid, by just touching the spheres between them, the ratio between the volume of one sphere and the volume of the grid's Voronoi cell is a measure of space filling, known as "covering radius". There is a superior limit for the covering radius in each dimension. The grid (or "lattice") having this radius is called the compact lattice, it is possible to have several lattices with the maximum covering radius.

**Reciprocal Grid:** A grid can be defined by using a vector basis  $\{\bar{v}_i\}$ , so that the relative position between two grid points is always a linear combination of the basis vectors with integer coefficients (diophantine equation)[4]. The grid defined by the basis  $\{\bar{v}_i\}$  has a reciprocal grid generated by the vector basis  $\{\bar{u}_i\}$  orthonormal to  $\{\bar{v}_i\}$ . It can be calculated by forming a matrix  $A$  whose columns are the basis vectors, and taking its pseudo-inverse  $B$ :

$$A = \{\bar{v}_i\} \quad B = A(A^T A)^{-1} \quad \{\bar{u}_i\} = B$$

The basis  $\{\bar{u}_i\}$  is called the dual basis of  $\{\bar{v}_i\}$ . The volume of the Voronoi cell can be calculated by taking the determinant of the  $A$  matrix.

The multidimensional Fourier Transform of a distribution of dirac deltas placed on the grid points, is a distribution of dirac deltas placed on the reciprocal grid points. This property is extensively used in cristallography to rely diffraction images of cristals with its lattice structure.

## 2.2 Topology definition on the grid

Topological characteristics of discrete grids become very important when tasks such as object recognition and extraction are faced. Great efforts are made to define correct topologies over discrete structures [12][2][10][9], particularly in the image processing community. The two main approaches (which can give rise to similar topologies) are:

- a) The assimilation of the discrete grid to a  $K$ -complex structure,
- b) The definition of discrete neighborhoods in each grid point.

The first approach is considered in this work since it provides a clear image of the grid geometrical properties.

### 2.3 $K$ -complex definition

A  $N$ -cell is a set whose interior is homeomorphic to the  $N$ -D disc:

$$D^n = \{\bar{x} \in \mathbb{R}^n : \|\bar{x}\| < 1\}$$

with the additional property that its boundary or frontier must be divided into a finite number of lower-dimensional cells, called the faces of the  $N$ -cell. A 0-D cell is a point, a 1-D cell is a line segment, a 2-D cell is a polygon and a 3-D cell is a polyhedron [9].

A  $K$ -complex is a finite set of cells:  $K = \bigcup \{\sigma : \sigma \text{ is a cell}\}$ , such that:

1. if  $\sigma$  is a cell in  $K$ , then all faces of  $\sigma$  are elements of  $K$ .
2. if  $\sigma$  and  $\tau$  are cells in  $K$ , then  $\text{Interior}(\sigma) \cap \text{Interior}(\tau) = \phi$ .

The dimension of  $K$  is the dimension of the highest dimension cell.

### 2.4 Discrete grid as a $K$ -complex

To define a  $K$ -complex over a  $N$ -D discrete grid, Voronoi cells of the grid are taken as  $N$ -cells. Their  $(N-1)$ -D frontiers are  $(N-1)$ -cells and so on.

To achieve a contour extraction, the sampling grid points should be segmented first. The segmentation classifies each point as being "object" or "background" (and so classifies the associated  $N$ -cells). The contour extraction consists in tracking the  $(N-1)$ -cells between "object" and "background"  $N$ -cells. This collection of  $(N-1)$ -cells can be used to build a  $(N-1)D$  "contour"  $K$ -complex, by adding all the lower dimensional cells of the original  $K$ -complex which are neighbors of the contour  $(N-1)$ -cells.

The great advantage of the compact grid topology, (that we have verified in dimensions two to four), is that the  $(N-2)$ -cells joint always  $(N)$ -cells in number of three, and their three  $(N-1)$ -dimensional frontier cells too. This arrangement guaranties that a binary segmentation of the  $N$ -cells will produce only two contour  $(N-1)$ -cells joined at the same  $(N-2)$ -cell. This property simplifies the cell connection process, since no ambiguity is possible in the  $(N-2)$ -cells.

The  $\mathbb{Z}^n$  grid can also define a  $K$ -complex topology, however it has  $(N-2)$ -cells which joint four  $(N)$ -cells with their four  $(N-1)$ -cells leading to a well known ambiguity in the contour extraction process when two diagonally opposed  $(N)$ -cells belong to "object" and the other two to "background".

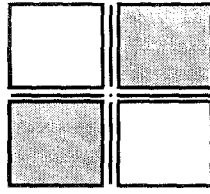


Fig. 1. Ambiguous case in  $\mathbb{Z}^n$  grid topology

**2-D topology** The topology of the compact 2-D grid is obtained from the  $K$ -complex built by taking the hexagonal Voronoi cells as 2-cells, line segments between two hexagonal cells as 1-cells and points at vertex of the hexagonal cells as 0-cells. It should be recalled that the hexagonal grid is its own reciprocal (following the definition in section 2.1), so the topology of the optimal sampling grid is the same of the compact grid. Contour extraction is simplified because at every 0-cell, only two of the three adjacent 1-cells can belong to contour.

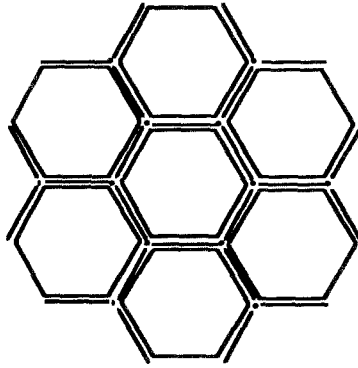


Fig. 2.  $K$ -complex associated to the compact 2-D grid

**3-D grid topology** The 3-D compact grid is the face-centered cubic lattice (FCC), which generates a  $K$ -complex whose 3-cells are rhombic dodecahedrons (Figure 3-a) [7][3], and as mentioned above, they joint at their edges in number of three. The dihedral angle of the faces is  $120^\circ$ . The rhombic dodecahedron faces, edges and vertex define respectively the 2-cells, 1-cells and 0-cells of the  $K$ -complex.

The reciprocal of the compact FCC grid is the body-centered cubic lattice (BCC), whose Voronoi cells are truncated octahedrons (Figure 3-b). The  $K$ -complex is built by taking the truncated octahedrons as 3-cells, and its faces, edges and vertex respectively as 2-cells, 1-cells, and 0-cells. The truncated octahedron has six square faces and eight regular hexagonal faces, It edges joint always two hexagons and a square (in the space filling structure). Truncated octahedron can be replicated to fill the 3-D space with the property of joining three polyhedrons at each edge. Its dihedral angles are  $109.47^\circ$  between two hexagonal faces, and  $125.26^\circ$  between the square and hexagonal faces.



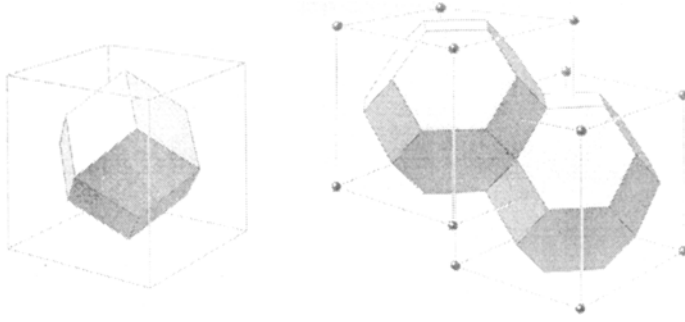


Fig. 3. Rhombic dodecahedron (a), Truncated Octahedron (b)

The  $K$ -complex topology associated to the BCC and FCC lattices can then be used to simplify the surface extraction process from 3D binary segmented data.

**4-D grid topology** The 4-D compact grid has a 4-D Voronoi cell formed by twenty 3-D rhombohedra, with 6 rhombic 2-D faces each one. A  $K$ -complex topology is defined using this 4-D Voronoi cell as 4-cells, rhombohedra as 3-cells, rhombic faces as 2-D cells, and so on. A rhombohedra is common to exactly three grid points, this lets also to track a 3-D  $K$ -complex around a 4-D object segmented in the grid.

### 3 Signal Processing Analysis

The Shannon theorem states the correct sampling rate for one-dimensional band-limited continuous signals by considering the interaction of their spectra in the frequency domain [1][11]. The recommended sampling rate is the double of the maximum frequency of the signal. A lower sampling rate will loss information, while a higher sampling rate will introduce redundancy.

The process of sampling a signal with a grid, corresponds in the spectral domain, to convolve the signal spectrum with the reciprocal of the sampling grid (defined in section 2.1). Considering signals with isotropic properties, that is, having spectra with a multidimensional spherical support, it is possible to assimilate the sampling process to a spherical packing problem in the multidimensional frequency domain.

Multidimensional spherical supported spectra must be replicated in the frequency domain by just touching the supports between them. Superimposed supports will give rise to aliasing problems, while vacuum space in the frequency domain will represent oversampling (redundancy). The optimal filling of the frequency domain is the fundamental condition to obtain a non-redundant sampling of the signal.

The problem of packing spheres compactly in regular lattices is well known [5][6]. The solution for the 2- $D$  case is the hexagonal lattice, and for the 3- $D$  case is the FCC lattice [3]. From the solid state point of view the  $\mathbb{Z}^n$  sampling grid is associated to the simple cubic lattice.

The optimal sampling grid is defined here as the reciprocal of the compact grid. This choice leads to obtain the maximum covering radius in the frequency domain and hence reduce the redundancy to its minimum value [11]. The compact grid size is adjusted to the signal maximum frequency  $F_c$ , to have a compact grid with a nearest neighborhood distance of  $2F_c$ . Therefore, the nearest neighborhood distance of the sampling grid is  $1/(2F_c)$ .

### 3.1 1-D sampling

A 1-D signal having a spectrum with maximum frequency  $F_c$ , that is, a support  $[-F_c, F_c]$  can be optimally sampled by using a grid of period  $1/2F_c$ . The spectrum support is the 1-D sphere of radius  $R = F_c$ , whose volume is  $2R$ . The Voronoi cell of the  $\mathbb{Z}^1$  sampling grid is the segment  $[-R, R]$  which has a volume  $2R$ . The compact lattice in  $\mathbb{R}^1$  space is the same  $\mathbb{Z}^1$  grid, so the volume of the compact Voronoi cell is  $2R$ .

Then, the covering radius in the 1-D case is 100%, which lets sample the signal without loss of information nor redundancy.

### 3.2 2-D sampling

A 2-D signal having a spectrum with maximum frequency  $F_c$ , has as spectral support the circle of radius  $R = F_c$  with volume  $\pi R^2$ . The  $\mathbb{Z}^2$  grid has a Voronoi cell of volume  $4R^2$ , then a covering radius of  $\pi/4 \approx 78.53\%$ .

The compact 2-D lattice is the hexagonal grid, defined by the base:

$$\bar{v}_0 = [1, 0] \quad \bar{v}_1 = [\sqrt{3}/2, 1/2]$$

The reciprocal grid is defined by:

$$\bar{u}_0 = [0, 2\sqrt{3}/3] \quad \bar{u}_1 = [1, -\sqrt{3}/3]$$

which also generates an hexagonal grid.

The Voronoi cell of the hexagonal grid with an inscribed circle of radius  $R$ , has a volume of  $2\sqrt{3}R^2$ , with a covering radius of  $\sqrt{3}\pi/6 \approx 90.69\%$ .

The ratio between the covering radius of the  $\mathbb{Z}^2$  grid and the hexagonal grid is  $\sqrt{3}/2 \approx 0.8660$  [6] which means that the number of samples of the reciprocal hexagonal lattice is the 86.60% of the number of samples needed in the  $\mathbb{Z}^2$  grid, when both sample the signal without information losses.

### 3.3 3-D sampling

A band-limited isotropic 3-D signal with maximum frequency  $F_c$  has a sphere of radius  $R = F_c$  as spectral support. The sphere volume is  $4\pi R^3/3$ , while the Voronoi cell of the  $\mathbb{Z}^3$  grid has a volume of  $8R^3$ , that is a covering radius of  $\pi/6 \approx 52.36\%$ .

The compact 3-D grid is the FCC lattice defined by the base:

$$\bar{v}_0 = [1/2, 1/2, 0] \quad \bar{v}_1 = [1/2, 0, 1/2] \quad \bar{v}_2 = [0, 1/2, 1/2]$$

Its reciprocal is the BCC lattice defined by the base:

$$\bar{u}_0 = [-1, -1, 1] \quad \bar{u}_1 = [-1, 1, -1] \quad \bar{u}_2 = [1, -1, -1]$$

The Voronoi cell of the FCC grid is the rhombic dodecahedron [7][3] of volume  $4\sqrt{2}R^3$ , with covering radius of  $\sqrt{2}\pi/6 \approx 74.04\%$ . The reciprocal of the FCC lattice is the BCC lattice, so the optimal grid to sample a 3-D signal is the BCC lattice with a nearest neighbor distance of  $1/(2F_c)$ .

The ratio between the covering radius of the  $\mathbb{Z}^3$  grid and the BCC grid is  $\sqrt{2}/2 \approx 0.7071$ , then the 3-D signal sampled with the BCC grid has the 70.71% of the number of samples needed in the  $\mathbb{Z}^3$  grid.

### 3.4 4-D sampling

A 4-D signal with maximum frequency  $F_c$  has a 4-D sphere of radius  $R = F_c$  as support. The sphere volume is  $\pi^2 R^4/2$ . The Voronoi cell of the  $\mathbb{Z}^4$  grid is the 4-D cube of side  $2R$ , with volume  $16R^4$ , which gives a covering radius of  $\pi^2/32 \approx 30.84\%$ .

The compact 4-D grid can be constructed based on the 3-D grid as:

$$\begin{aligned}\bar{v}_0 &= [1/2, 1/2, 0, 0] & \bar{v}_1 &= [1/2, 0, 1/2, 0] \\ \bar{v}_2 &= [0, 1/2, 1/2, 0] & \bar{v}_3 &= [1/4, 1/4, 1/4, \sqrt{5}/4]\end{aligned}$$

The corresponding dual basis is:

$$\begin{aligned}\bar{v}_0 &= [1, 1, -1, -\sqrt{5}/5] & \bar{v}_1 &= [1, -1, 1, -\sqrt{5}/5] \\ \bar{v}_2 &= [-1, 1, 1, -\sqrt{5}/5] & \bar{v}_3 &= [0, 0, 0, 4\sqrt{5}/5]\end{aligned}$$

It should be noted that a rotation of the basis vector is also a valid basis, and so it is possible to find several forms for the basis of the same grid.

The 4-D compact grid has a Voronoi cell of volume  $4\sqrt{5}R^4$  which done a covering radius of  $\sqrt{5}\pi^2/40 \approx 55.17\%$ . The ratio between the two grids is  $\sqrt{5}/4$ , what means that the optimal grid has the 55.90% of samples of the  $Z^4$  grid.

Table 1. summarizes the basic relations of the  $\mathbb{Z}^n$  sampling grid against the compact grid for dimensions one to four. Emphasize should be made about the progressive reduction of the covering radius as space dimension grows, making more relevant the use of compact grids. The cube volume and the compact voronoi cell volume are calculated for the appropriated scale to have an inscribed sphere of radius R.

	1-D	2-D	3-D	4-D
Sphere Volume	$2R$	$\pi R^2$	$4\pi R^3/3$	$\pi^2 R^4/2$
Cube Volume	$2R$	$4R^2$	$8R^3$	$16R^4$
Compact Voronoi cell volume	$2R$	$2\sqrt{3}R^2$	$4\sqrt{2}R^3$	$4\sqrt{5}R^4$
$\mathbb{Z}^n$ covering	100 %	78.53 %	52.36 %	30.84 %
Compact covering	100 %	90.69 %	74.04 %	55.17 %
$\mathbb{Z}^n$ / Compact	100 %	86.60 %	70.71 %	55.90 %

Table 1. Space covering relations for 1-D to 4-D grids

## 4 Application: Surface extraction from volume data

A Surface extraction algorithm is detailed here for the FCC lattice and its reciprocal, the BCC lattice; both endowed with a  $K$ -complex topology. Algorithm's global scheme is inspired from the classical "Marching Cubes Algorithm" [13]. The subjacent topology mentioned above is used to guide the connection between faces. The objective is to extract the surface of a segmented object in the volume data. Grid points are represented by its voronoi cell, while surface points are represented by the faces of voronoi cells.

The algorithm starts with a detection step in which all the voronoi cells are tested to find "object" cells adjacents to "background" cells. Surface points  $p_i$  are located along the line joining the pair of cells. In a second step, the surface points  $p_i$  should be connected between them to generate a 2-D  $K$ -complex. This connection is achieved following the neighborhood relations of faces in the  $K$ -complex structure.

Two surface points  $p_i$  would be connected if the associated faces of the voronoi cell have an edge in common in the space filling structure.

**Compact grid** The  $K$ -complex topology for the compact grid has rhombic dodecahedrons as 3-cells. When this polyhedron is replicated to fill the 3D space, each rhombic face has eight neighbor faces, two at each of its four sides. If a face belong to the surface, only one of the two faces joined at the same side could belong to the surface (since the 3-cell segmentation is binary). This reduce the connection process to the test of eight potential links at each surface point  $p_i$

In the implementation, a code is assigned to each  $p_i$ , this code represents the geometrical position of its associated face in the voronoi cell polyhedron. A table of neighborhoods is used to select the faces in the  $K$ -complex structure that should be tested. If a tested face belongs to the surface too, a link is set between the points associated to the pair of faces.

**Reciprocal of the compact grid** The  $K$ -complex topology for the reciprocal compact grid has truncated octahedrons as 3-cells. Whose faces are six squares and eight regular hexagons [7][3]. When this polyhedron is replicated to fill the 3D space, the hexagonal faces have twelve neighbor faces (at each side there are one hexagonal and one square face joined), and the square faces have eight neighbor faces (two hexagonal faces at each side).

The points  $p_i$  found in the detection step, receive a code corresponding to the geometrical position of its associated face in the voronoi cell. A table of neighbor faces in the  $K$ -complex are used to select the faces that should be tested. If a neighbor face belongs to the surface, the points associated to each one of the faces are linked.

**Triangulation** The connection step produces a 2-D  $K$ -complex which represents the object's surface. It is interesting to modify this structure and built a triangulation on it. Especially, for rendering and manipulation purposes. This is achieved by searching all the non-triangular 2-cells, and adding 1-cells between its 0-cells, to form triangles inside.

## 5 Results

The surface extraction method has been tested on a medical volume data. The original volume is a pubic bone CT scan sampled with a  $\mathbb{Z}^3$  grid. To test the proposed optimal grids, they have been built from the  $\mathbb{Z}^3$  grid by adding sampling points [3]. Figure 4. shows the rendering of surfaces extracted from the volume. At left the BCC grid is used. At right the FCC grid is used.

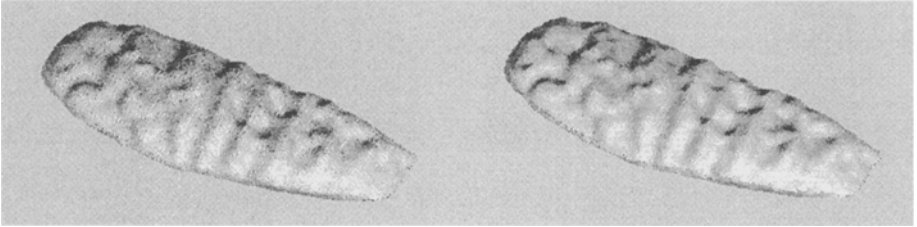


Fig. 4. Surface from oversampled Optimal grid (left), Reciprocal optimal grid (right)

The addition of point to the sampling grid oversamples the signal, so in the tests, the same CT scan has been resampled at the theoretical optimal density of each grid, the surfaces extracted are shown in Figure 5.



Fig. 5. Surface from adapted sampled Optimal grid (left), Reciprocal optimal grid (right)

Artifacts remaining from the sampling grid are consequence of the method used to estimate the nodes positions (a simply linear interpolation between the two concerned grid points). Actually, B-spline cubic interpolation is used, based on the original CT scan volume data, which generates smoother surfaces.

## 6 Discussion

Two objections are usually made on the use of other grids than the  $\mathbb{Z}^n$  one. The first is that original data are normally represented on a  $\mathbb{Z}^n$  grid, the second is the computational simplicity offered by the  $\mathbb{Z}^n$  grid.

The first argument is valid in general when the data acquisition device uses a  $\mathbb{Z}^n$  sampling, and then a resampling (by an interpolation reconstruction) is

needed to convert to another grid. However, in the particular case of Computer Tomography, the volume data is the result of a reconstruction from projections which has been made over a  $\mathbb{Z}^3$  grid only for simplicity reasons. Results presented in this paper, shows that it is interesting to develop reconstruction algorithms over optimal grids (BCC or FCC lattices) because they provide spectral and topological advantages.

The second argument, is limited to the application. It is obvious that data access is simpler in the  $\mathbb{Z}^n$  grid, but topology based applications will be simpler on the optimal and the reciprocal optimal grid, (the surface tracking shown here is an example). In particular, mathematical morphology operations have a better digital representation on the compact grid than on the  $\mathbb{Z}^n$  grid [14]. For this reason the compact grid is the preferred choice in this field [15].

## 7 Conclusion

Sampling grids with optimal topological and spectral properties have been determined here for 2D, 3D and 4D spaces. These grids are based on the spherical packing concept. The proposed grids optimize the density of points needed to sample a band-limited signal without loss of information. The use of the BCC lattice is recommended as the optimal sampling grid in 3D space. This grid optimizes the spectral occupation (minimize redundancy), and supports a coherent topology.

The FCC lattice, gives a lower spectral occupation than the BCC lattice (greater than that of the  $\mathbb{Z}^n$  grid, anyway), but offers a simpler topology, which in certain applications could be more important. A simple algorithm of surface extraction has been derived for 3D volume data, over the optimal grid and its reciprocal.

## References

1. A.Rosenfeld, A. Kak *Digital picture processing* Academic Press Inc. 1982.
2. J.K.Udupa, G.T.Herman *3-D Imaging in Medicine* CRC Press, 1989.
3. C.Kittel *Introduction to solid-state physics* John Wiley & Sons Inc. 1971.
4. D.Schwarzenbach *Cristalographie* Presses polytechniques et universitaires romandes, 1993.
5. J.H.Conway, N.J.A.Sloane *Sphere packing lattice and groups* Second edition, Springer-Verlag, A series of comprehensive studies in mathematics. 1993.
6. H.S.M.Coxeter *Introduction to Geometry* second edition John Wiley & Sons Inc. 1969.
7. K.Miyazaki *An adventure in multidimensional space* A Wile Inter-science publication, John Wiley & Sons Inc. 1983

8. E.Viterbo, E.Biglieri *Computing the voronoi cell of a lattice: the diamond-cutting algorithm* IEEE transactions on information theory; Vol 42, No. 1, January 1996.
9. L.C.Kinsey *Topology of surfaces* Undergraduate Texts in Mathematics, Spriger-Verlag, New York, 1993.
10. V.Kovalevsky *Shape in picture, a mathematical description of shape in gray levels images.* Springer-Verlag; NATO ASI series, Series F: Computer and systems science Vol 126. 1992.
11. D.E.Dudgeon, R.M. Mersereau *Multidimensional digital signal processing* Prentice-Hall, Englwood Cliffs; NJ; 1984.
12. D.Nogly, M.Schladt *Digital Topology on Graphs* Computer Vision and Image Understanding, Vol 63, No. 2; March; pp 394-396, 1996.
13. W.E. Lorensen, H.E. Cline *Marching Cubes: A high resolution 3D surface construction algorithm* Computer Graphics, Vol 21, No. 4, Jul 1987. pp 163-169.
14. E.R. Dougherty *Mathematical Morphology in image processing.* Marcel Dekker, New York 1991.
15. J.Serra *Image Analysis and Mathematical Morphology* . Academic Press Inc. 1982